

Estimation of annual forest evapotranspiration from a coniferous plantation watershed in Japan (2): Comparison of eddy covariance, water budget and sap-flow plus interception loss



Takanori Shimizu^{a,*}, Tomo'omi Kumagai^b, Masahiro Kobayashi^a, Koji Tamai^a, Shin'ichi Iida^a, Naoki Kabeya^c, Reo Ikawa^d, Makiko Tateishi^{e,f}, Yoshiyuki Miyazawa^{g,h}, Akira Shimizu^c

^a Forestry and Forest Products Research Institute, Matsunosato, Tsukuba, Ibaraki 305-8687, Japan

^b Hydrospheric Atmospheric Research Center, Nagoya University, Chikusa-ku, Nagoya 464-8601, Japan

^c Kyushu Research Center, Forestry and Forest Products Research Institute, Kurokami, Kumamoto 860-0862, Japan

^d Geological Survey of Japan, AIST Tsukuba Central 7, Tsukuba, Ibaraki 305-8567, Japan

^e Kasuya Research Forest, Kyushu University, Sasaguri, Fukuoka 811-2415, Japan

^f Graduate School of Agriculture, Kyoto University, Kitashirakawa, Sakyo-ku, Kyoto 606-8502, Japan

^g Research Institute for East Asia Environments, Kyushu University, Motoooka, Fukuoka 811-0395, Japan

^h Department of Geography, University of Hawaii at Manoa, 2424 Maile way, Honolulu, Hawaii, 96822, United States

ARTICLE INFO

Article history:

Received 30 November 2013

Received in revised form 12 December 2014

Accepted 13 December 2014

Available online 23 December 2014

This manuscript was handled by

Konstantine P. Georgakakos, Editor-in-Chief

Keywords:

Multi-method comparison

Patchy planted forest

Stand level flux

Water vapor exchange

SUMMARY

Evapotranspiration (ET) was estimated from a planted coniferous forest in southwestern Japan by applying three methods: the eddy covariance method; the measurement of rainfall (P) and runoff (Q) in a small watershed; and a combination of rainfall interception loss (I_C), upper canopy transpiration based on a sap-flux density measurement in Japanese cedar (*Cryptomeria Japonica* D. Don) stands (E_{UC}), and modeled sub-canopy ET (E_{SC}). After inverse multiplication of the energy imbalance ratio, ET by the eddy covariance method (ET_{EC}) was 839.9 mm in 2007 and 811.8 mm in 2008. The yearly values of $P-Q$ were partially affected by P in the previous autumn. After continuous data collection for more than 5 years, $P-Q$ became stable. The 9-year (2000–2008) average $P-Q$, which was considered most reliable in this study, was 897.5 mm y^{-1} . The cumulative ET_{EC} during the daylight hours from the right stream bank, covered mainly with large Japanese cedars, was 894.1 mm from April 2007 to March 2008. The value was almost the same as that calculated as the components sum ($ET_{COMP} = I_C + E_{UC} + E_{SC}$: 911.4 mm), and the comparison suggested that the annual totals of ET_{EC} with an energy imbalance correction provide a reliable estimate of ET in a forest stand on a complex topography. Spatial variation in the watershed was likely caused by differences in soil water retention at each slope position. The slight difference in annual ET_{EC} in 2007 compared with 2008 was attributed to differences in the radiative energy input. In the monthly-weekly analysis, ET_{COMP} was frequently higher than ET_{EC} after heavy rainfall, while ET_{EC} was higher under dry conditions and during active ET. Even under dry canopy conditions, daily ET_{EC} was often higher than $E_{UC} + E_{SC}$. The results suggested a time-lag in evaporation from the ecosystem and/or under-estimated ET_{EC} after rainfall.

© 2014 Elsevier B.V. All rights reserved.

1. Introduction

Japan's mountainous topography and the patchiness of the vegetation make it difficult to estimate water and nutrient balances and cycles within and throughout the forest ecosystem. Water is the most significant natural resource on the earth, and ET from

forests is one of the most significant factors influencing the water cycle.

Japanese cedar (*Cryptomeria Japonica* D. Don) and Japanese cypress (*Chamaecyparis obtusa* Endl.) are the most popular planted species in Japan, and cover 12% and 7% of the land surface of the country, respectively (Forestry Agency of Japan, 2013). These species were often planted in areas with the same slope but on different slope positions. Japanese cedar was usually planted from valleys to lower hillsides with relatively wet and fertile soils, while Japanese cypress was usually planted on the drier and more

* Corresponding author at: Forestry and Forest Products Research Institute, 1 Matsunosato, Tsukuba, Ibaraki 305-8687, Japan. Tel.: +81 29 829 8234; fax: +81 29 874 3720.

E-mail address: simizuta@affrc.go.jp (T. Shimizu).

nutrient poor ridge areas (Yamashita et al., 2004). Accordingly, these two species often have significantly different potential capacities for growth, and as a result evapotranspiration (ET: See Table 1 for a full list of abbreviations) and carbon assimilation may be variable in the two species. Furthermore, Japan's planted coniferous forests often grow in mountainous terrain and a portion of these forest stands have been modified by vigorous growth of the original vegetative species present, e.g., evergreen and/or deciduous broad-leaved species. As a result, over time such forests have come to include more patchy areas than previously expected rather than maturing into monocultures of the original plantation species; this has resulted in wide variation in growth rates caused by each site's microsite conditions.

Rainfall (P) and runoff (Q) amounts have been measured in watersheds of various sizes and with different vegetation types worldwide (e.g., Zhang et al., 2001). The average of the residual values ($P-Q$) have been compared, based on the assumption that $P-Q$ was equal to ET (e.g., Zhang et al., 2001; Komatsu et al., 2008). Several years' data are required to obtain reliable $P-Q$ values because a single year may be affected by the water storage from the previous year, rainfall intensity of the current year, and/or antecedent rainfall in the last several years (e.g., McGlynn et al., 2003). To determine a sufficient duration of measurement of P and Q for reliable estimation of ET, a long-term and continuous dataset is needed, as the numbers of years required may vary with the topography, geology and meteorological conditions at the site. Furthermore, recent research in some forest watersheds has suggested that underflow around runoff measurement gauges could occur (Waichler et al., 2005) and that bedrock infiltration was not negligible (Katsuyama et al., 2010). Thus, the results of rainfall-runoff observation ($P-Q$), which are believed to provide a robust estimation of ET, should be reexamined carefully through comparison with other observations conducted simultaneously, prior to their use in further analyses.

Eddy covariance technique (EC) has been a powerful tool especially in this century used not only to examine the results of P and Q measurement, but also to grasp the details of variation in ET (e.g. Wilson et al., 2001; Barr et al., 2012; Domec et al., 2012). Kosugi et al. (2007) estimated ET_{EC} (ET based on the eddy covariance measurement) for a single-species (Japanese cypress) plantation forest in a small watershed in central Japan and Matsumoto et al. (2011) presented the results of subsequent research with an extended observational period. Subsequently, Kosugi and Katsuyama (2007) compared their ET_{EC} with the results of P and Q measurements, and showed the average annual ET_{EC} for 3 years was very close to the average 33-year water budget. As Kosugi et al. (2007) noted, and as is often the case in Japan, our target forest is located on mountainous topography. Moreover, our study site comprises patchy plantation forest, also a common feature in Japan as described above. These characteristics are not ideal for the application of the eddy covariance method and thus the results should be examined with particular care.

Another powerful method used to estimate upper canopy transpiration (E_{UC}) is sap-flux density (F_d) measurement, which is not affected by topographical complexity. Additionally, E_{UC} data are often combined with measured or modeled interception loss (I_C), for ET estimation. Ford et al. (2007) applied a combination of E_{UC} from F_d measurement from 40 trees and modeled I_C as the ET of a white pine plantation forest. Comparing the total value with P and Q measurement, they confirmed the result of Wilson et al. (2001), showing that $P-Q$ created a higher estimation of ET than their measurement using $E_{UC} + I_C$. Holst et al. (2010) obtained E_{UC} from the sap flux measurements of 12 trees in a beech forest stand. They obtained the parameters of two water budget models, which reproduced the soil water dynamics quite well overall, but the degree of fit depended on the year and season. Oishi et al. (2008) measured F_d of a total 40 trees from dry and wet plots, and carefully extended the results to estimate E_{UC} at a larger scale, using

Table 1
List of abbreviations with definitions and units.

Abbreviation	Definition	Unit
C_{IB}	Monthly energy balance ratio	
D	Vapor pressure deficit at the height of 42 m	kPa
ET	Evapotranspiration from the site	mm time ⁻¹
ET_{COMP}	ET estimated from the sum of $I_C + E_{UC} + E_{SC}$	mm time ⁻¹
ET_{EC}	ET estimated from the eddy covariance method	mm time ⁻¹
$ET_{EC,C}$	ET_{EC} corrected by the monthly energy imbalance ratio (C_{IB})	mm time ⁻¹
$ET_{EC,NC}$	ET_{EC} without any correction	mm time ⁻¹
$ET_{EC,R}$	ET_{EC} calculated from the residual of energy budget equation ($Rn-G-H-S_H$)	mm time ⁻¹
E_{SC}	Sub-canopy transpiration from Japanese cedar stands, obtained by the model of Pearcy and Yang (1996)	mm time ⁻¹
E_{UC}	Upper canopy transpiration from Japanese cedar stands, obtained by the sap-flux measurement	mm time ⁻¹
$E_{UC,P}$	E_{UC} of certain plot	mm time ⁻¹
$E_{UC,P}$	E_{UC} of upper slope position in the right bank side	mm time ⁻¹
$E_{UC,LP}$	E_{UC} of lower slope position in the right bank side	mm time ⁻¹
F_d	Xylem sap flux density	m ³ m ⁻²
G	Ground heat flux, measured at the depth of 5 cm in the soil	W m ⁻¹
H	Sensible heat flux by the eddy covariance method	W m ⁻¹
I_C	Interception loss calculated by $P-T_F-S_F$	mm time ⁻¹
P	Gross rainfall measured	mm time ⁻¹
Q	Runoff from watershed	mm time ⁻¹
Q_{WS2}	Q from WS (watershed) 2 in the objective site (KHEW)	mm time ⁻¹
Q_{WS3}	Q from WS (watershed) 3 in the objective site (KHEW)	mm time ⁻¹
q	Instantaneous flow rate	m ³ s ⁻¹
R_n	Net radiation measured at the height of 47.2 m	W m ⁻¹
S_d	Downward Solar radiation measured at the height of 47.2 m	W m ⁻¹
S_F	Stemflow measured at a particular plot	
S_H	Storage of sensible heat under the eddy covariance observation height	W m ⁻¹
$S_{v,E}$	Storage of latent under the eddy covariance observation height	W m ⁻¹
T_a	Air temperature measured at the height of 42 m	°C
T_F	Throughfall measured at a particular plot	mm time ⁻¹
Δ	Difference from one year to the next, calculated by subtracting the value of a month in 2007 from that of the same month in 2008	
λE	Latent heat flux by the eddy covariance method	W m ⁻¹
θ	Volumetric soil water content measured at a particular plot, averaged daily	m ³ m ⁻³
θ_{MAX}	Maximum θ measured at the plot during the measurement period	m ³ m ⁻³

intensively collected allometric information. They found the total of E_{UC} , the measured I_C and modeled forest floor evaporation (E_F) agreed well with estimates based on ET_{EC} , especially on an annual basis. Meanwhile, monthly estimation was generally higher in summer and lower in winter than ET_{EC} . Based on these results, the total of ET components ($= E_{UC} + I_C + E_F$) would be reliable for estimating ET for periods of several months to annually. However, the daily-monthly variation of E_{COMP} should be cross-checked with other methods.

In the preceding paper (Kumagai et al., 2014; hereafter Kuma14), we conducted F_d measurement for a total 57 trees to estimate E_{UC} along with continuous measurement of I_C , and combined them with the modeled sub-canopy transpiration (E_{SC}). The result was considered a robust estimate of annual ET in the Japanese cedar forest stand, even though the data had been acquired in complex terrain. Therefore, if possible, the annual ET_{EC} should be tested through the comparison with $ET_{COMP} = E_{UC} + E_{SC} + I_C$, since the EC method contains uncertainty when applied to complex terrain. Furthermore, the seasonal variation of the ET_{COMP} should be compared with ET_{EC} to examine the consistencies and differences in ET estimation by both methods.

In the present paper, we initially check the certainty and limitation of the supposition that the value of $P-Q$ we obtained represents watershed ET, and compared the water budget with ET_{EC} . Second, we compare the downscaled ET_{EC} with the result of Kuma14. Taking the opposite direction of Oishi et al. (2008), the process of examining whether ET_{EC} obtained on a forest with complex terrain can represent the stand scale ET proved challenging. We divide ET_{EC} data into two wind sectors, one of which mainly comprises a Japanese cedar plantation. The estimated ET_{EC} from the sector is compared with ET_{COMP} from the Japanese cedar stand. Through these comparisons, we show the applicability and reliability of ET_{EC} as an estimate of ET for a forest watershed with complex terrain, as well as on the stand scale. Furthermore, to examine the applicability of ET_{EC} to estimate seasonal variation in ET in the same forest, we consider which environmental factors produce the observed yearly variation of ET_{EC} between 2007 and 2008, based on 2 years of data obtained from the multi-method observations.

2. Materials and methods

2.1. Study site and water budget measurement

Observations were conducted at the Kahoku Experimental Watershed (KHEW), one of the Asiaflux network sites located on Kyushu Island, southwestern Japan. The mean air temperature, annual mean precipitation and their standard deviations from 2000 to 2008 were 15.3 ± 0.28 °C and 2138 ± 364 mm, respectively. The observation site is underlain by crystalline schist and the complex topography includes many ridges and valleys. The thickness of soil surface layer is typically around 1 m, which becomes thinner (≈ 0.5 m) along ridges and in the bottom of the valley, and much thicker (≈ 4 m) in some parts of mid-slope (e.g., Ohnuki and Shimizu, 1998). The site was surrounded and covered by planted forest, excepting a golf course located 500 m northwest of the site.

The site consisted of three small watersheds, labeled as WS1, WS2 and WS3 and forest stands around them (Fig. 1). The area and elevation of these watersheds are 2.33 ha and 135–205 m a.s.l., 2.63 ha and 148–225 m a.s.l. and 3.69 ha and 157–255 m a.s.l., respectively. Water budget observation at KHEW was started in 1992 (Shimizu et al., 1994). In this study we mainly used the data from 2000 to 2008 and obtained from WS2 and WS3, since the stream flow data from WS1 was checked less frequently and thus less reliable because WS1 was a little more remote than WS2

and WS3 and no other instrument was installed in it. The prevailing daytime (or daylight hours) wind direction, which is mainly affected by the Southeast Asian monsoon, and is distorted by mountain-valley flow, typically blowing between southeast and southwest in summer and between northeast and northwest in winter. At night, the mountain-valley flow from a northeasterly direction often becomes dominant, especially as the winds approach calm conditions.

Planted conifers are the main overstorey vegetation of the site with Japanese cypress stands on the ridges and upper slopes, and with Japanese cedar growing from valley floor to middle of the hillside. Generally, the stand volume per unit area was higher in the latter than the former, implying that Japanese cedar was usually planted on sites richer in water and nutrients. As shown in Fig. 2 and Shimizu et al. (2003), Japanese cypress of various ages (30–52 years in 2007) are mainly planted and secondary broad-leaved species partially invade the larger part of the left stream bank of WS2 and WS3 except in the valley area. Meanwhile, from the right bank of WS2 to WS1, well-grown and even-aged Japanese cedar stands (52 years in 2007) were dominant and occupied the broad valleys. Shimizu et al. (2003) and Kuma14 provide details related to the vegetation in the watersheds, noting that a 7-year time-lag exists between the information described in the former and that in latter. As for understory vegetation, annual and perennial plants grew thickly under normal-sized Japanese cedar stands, while understory plants were relatively sparse under the Japanese cypress stands and large-sized Japanese cedar.

The valley side slopes are relatively steep in WS3 and the difference in elevation between the valley and the ridge is the largest among the three watersheds. In the 1990s, measurements related to the Bowen ratio energy balance (BREB) method were collected using two 22-m-tall observation towers, each of which was built in the Japanese cedar forest stand along the valley of WS3 (Shimizu et al., 2003).

A small concrete v-notch weir with a grit chamber was built at the end of each small watershed and a stainless-steel 60° v-notch was installed in the center of each weir. The water levels were measured using float level meters (HDR-115, Ikeda-keiki, Tokyo, Japan) and recorded data continuously mechanically. For all watersheds, the instantaneous runoff from the watersheds (q) was calculated by a power function of each. Then, Q was calculated from the time integration of q . The hydrologic year was tentatively set as the same calendar year, partly because for convenience, but mainly because P and Q were usually lower and stable around the beginning of the year.

Gross rainfall (P) was measured using a 0.5-mm tipping bucket type rainfall gauge (RT-5, Ikeda-Keiki, Tokyo, Japan). It was installed along an unpaved road near WS2 with a pulse count data recorder (HOBO H07, Onset Computer Corp., Bourne, MA, USA). The value of P in this study was calculated from the obtained data without any tipping bucket correction, since we did not carry out the examination for the rainfall gauge. However, when the correction function of Iida et al. (2012), which was obtained from the examination of another type of 0.5-mm rainfall gauge, was experimentally applied to our instrument and data, the difference between corrected and uncorrected annual P was 0.46% both 2007 and 2008.

2.2. Heat fluxes and meteorological factors

An over-canopy meteorological observation tower was built in the center of WS2 (Fig. 1). An albedo meter (CM14, Kipp & Zonen, Delft, Holland) and two pyrgeometers (CG3, Kipp & Zonen) were set at a height of 47.2 m to obtain upward and downward solar radiation and infra-red radiation, respectively. Their total was calculated as net radiation (R_n). Soil heat flux (G) was also obtained at

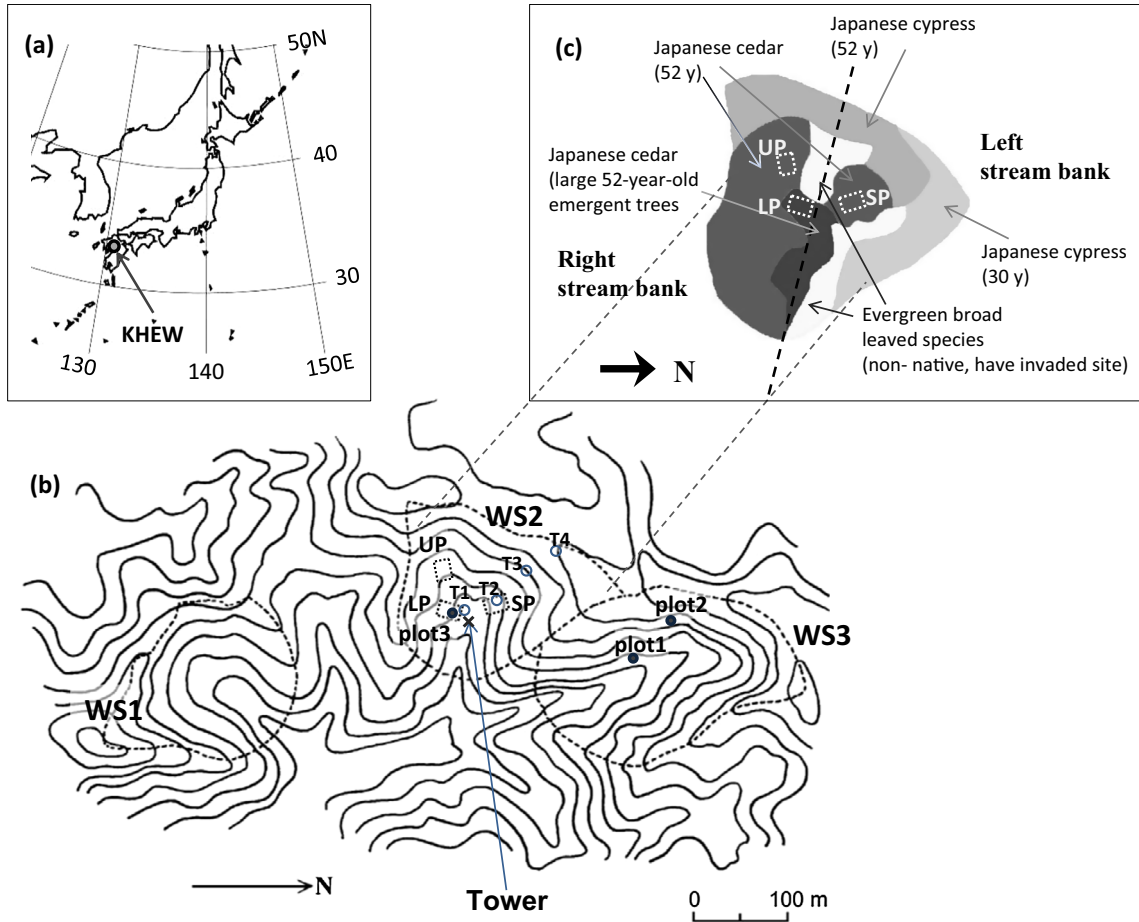


Fig. 1. (a) The location of the study site (KHEW). (b) Topographical map of the site. A 50-m height observation tower (cross mark), sap-flux and soil water measurement plots (dotted line squares of LP, UP and SP in the text), shallow soil water content measurement plot (T1, T2, T3 and T4), throughfall and stemflow measurement plots (closed circles of plots 1, 2 and 3 in the text) are also represented. (c) Vegetation map of WS2 in KHEW. The broken line divides the left (north) and the right (south) banks of WS2.

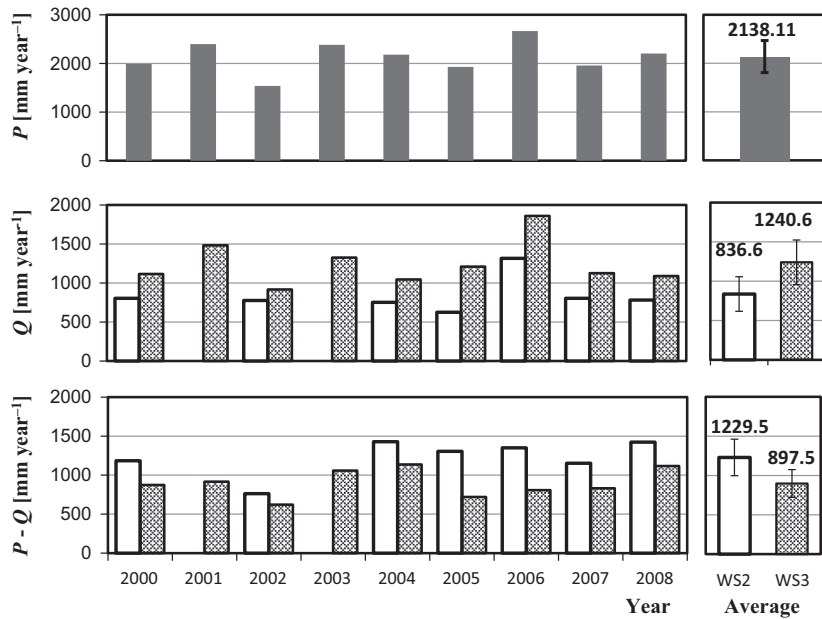


Fig. 2. Annual variations of rainfall (P : upper panel), runoff from WS2 and WS3 (Q_{WS2} and Q_{WS3} , white block and meshed block in the middle panel, respectively), and $P-Q_{WS2}$ and $P-Q_{WS3}$ (lower panel) for 2000–2008. The 9-year average values were also shown at the left side panels, with error bar of \pm S.D. (standard deviation).

0.05 m depth (including about 0.04 m litter material) near the tower with a heat flux plate (HFT 3.1, REBS, Seattle, WA, USA). A Barometer (PTB100, Vaisala, Helsinki, Finland) was installed at a height of 51.0 m, and two ventilated psychrometers (MH-020L, Eko instruments, Tokyo, Japan) measuring wet- and dry-bulb temperatures, set at the heights of 20 m and 42 m. to acquire air temperature and humidity. These values were applied to estimate temporal heat and water vapor storage in the air from the ground level to the EC measurement height. Using a dielectric aquameter sensor (EC-20, Decagon Devices, Inc., Pullman, WA), soil water content (θ) was measured in the three plots for sap-flux density measurement (LP, UP and SP in Fig. 1(b)) until May 2008 (see Kuma14), and at 5 cm depth at each of the four points (T1–T4 in Fig. 1b, see also Tamai et al., 2010). In this study, the depth weighted average θ obtained at plot SP was used for eddy covariance data interpolation. When comparing soil water content among sites, we used θ/θ_{MAX} instead of θ to account for instrumental error, where the subscript MAX means the maximum value in the observation period.

A sonic anemo-thermometer (SAT: DAT-600/TR-61C, Sonic: formerly Kaijo-denki, Tokyo, Japan) and a gas intake mouth were installed at the top of the tower (51.0 m), separated by 0.15 m. The tilt of the SAT was measured by a digital inclinometer (Pro360, Onset): The 0.3 degrees tilt was found only along the y-axis direction of the SAT. Based on analysis using similarity functions (e.g., Dyer, 1974) and turbulence data taken primarily from the right bank side, the zero plain displacement and the roughness length were calculated as 28.0 m and 5.3 m, respectively. Assuming these values were applicable to the entire watershed, 80% of the cumulative footprint was estimated at 191 m and 398 m from the tower under moderately unstable conditions ($L = -50$ m, where L is Obukhov length) and ideally neutral conditions, respectively. Estimation was made using the method of Hsieh et al. (2000). Sample air was drawn from the mouth to the closed-path infrared gas analyzer (IRGA: LI-7000, Li-Cor, Lincoln, NE, USA) through 57 m long Teflon tubes with a 6 mm inner diameter from the mouth to an intake pump and 3.5 m of 4 mm between the pump and IRGA. The normal flow rate was 7–8 L min⁻¹ and calibration was conducted about once per week by switching the flow paths of the sample gas and reference gas manually. Note that the closed-path sample had been dehumidified when using the previous version of IRGA (LI-6262, Li-Cor) until late 2006 (see Shimizu, 2007). Analog signals from the SAT and IRGAs were recorded at 10 Hz, using a data logger (DR-M3b, TEAC, Tokyo, Japan). To avoid the density effect (Webb et al., 1980), we applied mixing ratio of water vapor to dry air for flux calculation.

Average values and fluctuations of wind velocity components were calculated after correcting for SAT transducer shadow (Shimizu et al., 1999) and sonic tilt correction base on the inclinometer measurement, applying 30-min block averages, as well as scalars. During the day, eddy fluxes were calculated on the fixed coordinate system, which is referred to as the “ratio of moving averages of vertical/horizontal wind components” (Shimizu, submitted for publication). At night, eddy fluxes were determined using the sector-wise planar fit method (e.g., Siebicke et al., 2012). Prior to analysis, calculated fluxes were screened for quality control (QC) following a simple and strict method submitted by Foken et al. (2012). The value of friction velocity was not applied as a data screening threshold in this study, excepting the use of 0.2 m s⁻¹ to decrease the effect of the golf course at night when the wind direction was west-northwest. High frequency loss of closed-path H₂O variance would become more significant than theoretically expected especially that obtained under humid conditions (e.g. Ibrom et al., 2007). This was corrected by empirical equations similar to Ibrom et al. (2007); the detailed procedure was described elsewhere (Shimizu, submitted for publication).

The eddy covariance data applied to the analysis in this study were those obtained from January 2007 to December 2008. In the period, a data gap of more than 3 h occurred five times, but only in 2008: 13–15 January, 24 January–6 February, 2–4 July, 4–8 August and 18–25 November. The dataset was analyzed using two steps. First, to fill data gaps caused either by missing data or the strict QC guidelines, the multiple imputation method was applied (Hui et al., 2004) using NORM software (e.g., Iida et al., 2009). The values of R_n –G, downward shortwave radiation (S_d), SAT wind speed, air temperature (T_a) and vapor pressure deficit (D) measured at a height of 42 m, and daily θ at T2 (Fig. 1b) were used to interpolate the latent and sensible heat fluxes.

Gaps in the data obtained in daylight hours ($S_d > 0$) were filled using two types of gap-filling processes. In the first, gaps were filled after the dataset was divided by the wind direction, from right and left banks (Fig. 1c), after which ET_{EC} was estimated as the average of the interpolated ET of values from both stream banks. In the second method, gaps in the data were filled without categorizing by the wind direction. Gap-filling of nighttime data ($S_d = 0$) was carried out without dividing the data by the wind direction because less than 10% of the data passed the strict QC criteria. Thus, we assumed nighttime evaporation (sometimes condensation) was similar on both bank sides.

The gap-filling process was carried out for every 6 months of data. The multiple imputation method was applied twice during gap-filling. Using NORM software, the first gap-filling was performed on the highest class data (corresponding to class QC 1–3 in Foken et al., 2012). Raw data within 20% or 20 W m⁻² of the first dataset were then added to the highest class data and the gap-filling process was reiterated. Gap-filled datasets were used to calculate the correction coefficient of energy imbalance (C_{IB}), which is the inverse of the energy imbalance ratio, as shown in Eq. (1):

$$C_{IB} = \sum(R_n - G) / \sum(H + S_H + \lambda E + S_{\lambda E}), \quad (1)$$

where H and λE are sensible and latent heat fluxes, respectively, measured by the eddy covariance method; S_H and $S_{\lambda E}$ are changes of sensible and latent heats within the height of the eddy covariance measurement, estimated by air temperature and water vapor measured at the heights of 42 m and 20 m, respectively. Monthly C_{IB} was calculated separately, daylight hours and nighttime. In this paper the energy imbalance correction means that multiplying the relevant C_{IB} was done to both ($H + S_H$) and ($\lambda E + S_{\lambda E}$).

2.3. Canopy interception and vegetation transpiration

The interception loss (I_C) was calculated from January 2007 to May 2008, applying the measured throughfall (T_F) and stemflow (S_F) in the three plots instrumented in KHEW. Plots 1 and 2 were set in WS3 and plot 3 was in WS2 (Fig. 1). Note that continuous measurements could be conducted only in plot 1 because intermittent instrumental error occurred in plots 2 and 3; but the remaining data were applied to the discussion in the following section. The vegetation cover in plots 1 and 3 was Japanese cedar, while that of plot 2 was Japanese cypress. The average tree height and density measured in 2008 were 20.8, 14.4, and 29.9 m and about 1200, 1600 and 600 trees ha⁻¹ for plots 1, 2 and 3, respectively. In each plot, two 0.4–0.45 m² troughs made of hard PVC and connected to 0.2-L tipping bucket flow meters (UIZ-200, Uizin, Tokyo, Japan) collected the T_F water. Stemflow was collected with urethane rubber 3 cm thick, which was cut to incline from the outer to the inner side, that was wrapped around the tree trunks at about 1.2 m height and connected with a rubber tube; stemflow then flowed to 0.5-L tipping bucket flow meters (plot1: 500 cc model, Yokogawa Electric Corporation, Tokyo, Japan; plots 2 and 3: UIZ-500, Uizin). For plots 1, 2 and 3, the S_F was measured for four, four

and two trees and their total projected areas 21.4 m², 22.5 m² and 45.5 m², respectively. A pulse count data logger (HOBO H07, Onset) was set and the timestamp was recorded when each bucket tipped. The T_F and S_F were estimated through application of the tipping bucket correction, which is necessary when high water flow rates into the bucket occur (Iida et al., 2012). The Appendix presents the details of the correction carried out in this study. Rainfall losses by canopy interception (I_C) were estimated by the water budget equation using Eq. (2):

$$I_C = P - T_F - S_F. \quad (2)$$

Xylem sap flux density (F_d) measurements were conducted using the thermal dissipation method with Granier-type sensors (e.g., Granier, 1987). Kumagai et al. (2014) provide specifications of the sensor and the details of the measurement system. For F_d measurements, three plots were set in the Japanese cedar forest stands in WS2 (Fig. 1b and c). Two of the three plots, named UP and LP, were named the same in Kumagai et al. (2007): They were set on the right bank and located at the middle of the slope (UP) and near the valley (LP). The other plot, named SP, was located on the left bank, at the middle of a south-facing slope. The number of trees selected for the measurement of F_d were 23, 15, and 19 for plots UP, LP and SP, respectively (see Table 1 in Kuma14). F_d measurement data were obtained in all three plots from early March 2007 to late June 2008. Plot-based upper canopy transpiration ($E_{UC,P}$) was calculated from the sum of F_d multiplied by each sapwood area of each measured individual tree and then divided by the plot area. We calculated E_{UC} as the area-weighted average $E_{UC,P}$ of all three plots.

The YPLANT program (Pearcy and Yang, 1996) was used to estimate transpiration based on sub-canopy vegetation (E_{SC}). Kuma14 describes the details of the processes. Saplings of three selected species (*Quercus glauca* Thunb., *Castanopsis sieboldii* Hatsushima ex Yamazaki et Mashida, and *Eurya japonica* Thunb.) were sampled as typical understory vegetation and leaf gas exchange parameters were obtained. Furthermore, a three dimensional leaf distribution was reconstructed for the simulation based on the measurement of the sampled sapling architecture and the analysis of digital pictures. The LAI of the understory was set at 2.0 based on observations of leaf area density profiles, which corresponded to 40–50% of the total vegetation area index measured under the Japanese cedar stands using a plant-canopy analyzer (LAI-2000, Li-Cor). This information was applied to the YPLANT program and E_{SC} was calculated. Monthly calculation of E_{SC} was based on monthly measurements of leaf and canopy parameters taken during the day under sunny or cloudy conditions. In this study we used E_{SC} as an estimate of sub-canopy ET, assuming the reduction of transpiration in rainy conditions was balanced by forest floor evaporation.

3. Results and discussion

3.1. Reliability and limitation of annual ET estimation

3.1.1. ET from water budget measurement

Fig. 2 shows annual P and $P-Q$ for WS2 and WS3 ($P-Q_{WS2}$ and $P-Q_{WS3}$, respectively) from 2000 to 2008. The 9-year average P , Q_{WS2} and Q_{WS3} were 2138.1 mm, 836.6 mm and 1240.6 mm respectively, although the average Q_{WS2} was calculated without data from 2001 and 2003 because only partial data were available for Q_{WS2} data in those years. Consequently, the average $P-Q_{WS2}$ and $P-Q_{WS3}$ were 1229.5 mm and 897.5 mm, respectively. Based on the data compiled by Komatsu et al. (2008), the annual $P-Q$ at our site in southwestern Japan was considered at most 1100–1200 mm when annual P is less than 3000 mm. Thus, using $P-Q_{WS2}$ to estimate ET from the watershed probably resulted in an overestimate

of ET. From the comparison of 9-year daily Q_s , the trend Q_{WS2} being lower than Q_{WS3} was clearly confirmed as both Q_s increased when daily Q_s were less than 10 mm day⁻¹ (Fig. 3a). In contrast, Q_{WS2} was occasionally higher than Q_{WS3} when Q_{WS3} was greater than 10 mm day⁻¹ (Fig. 3b). In both cases, Q_{WS2} and Q_{WS3} were well-correlated, and the difference between Q_{WS2} and Q_{WS3} can be estimated using the polynomial equations in Fig. 3. This result suggests that water leakage from deep soil and/or by bedrock infiltration was much greater at WS2 than at WS3, assuming an insignificant difference in ET between the two watersheds. Ikawa (2008) explained the difference could be attributed to the orientation of the schistosity plane that was inclined from northwest to southeast: the direction of the plane crosses the valley in WS2, allowing deep ground water near the water table pass through the watershed boundary. In addition, the majority of baseflow discharge and leakage loss may be controlled at the same spot in WS2 (Fig. 3a). From a topographical perspective, a broad inflection point exists in the valley of WS2 near the tower where soil water may concentrate and stagnate, and streamflow in WS2 is located just downstream of that point. Lateral flow toward the valley and gravity flow toward the water table are likely to occur there, and the latter might become a source of leakage. In WS3, because the plane is almost perfectly aligned with the direction of stream flow and the valley has uniform and steep slant, underground water tends to gather toward the downstream end of the watershed.

Although $P-Q_{WS3}$ was closer to published ET values than $P-Q_{WS2}$ (see Kuma14), the annual variation in $P-Q_{WS3}$ was greater than expected. Yearly Q values were dependent on P values in the same period (Fig. 4), and were also influenced by the magnitude of the preceding year's P . From the comparison of Q_{WS3} in January–December with P in 12 months preceding the P period by a monthly step, the best correlation was found when P was allowed to lag by 4 months (P from September–August and Q_{WS3} from January–December; Fig. 4(b)). This does not suggest that Q consisted primarily of the preceding 4 months' P . Rather, after the dry soil conditions of summer and early-middle autumn, P in late autumn and early winter tended to contribute to soil water storage. If a volume of stored soil water is large, it results in higher baseflow, which then causes higher Q/P in the following season. Moreover, the stability of P each year in January–March in KHEW during the 9 years (max: 327 mm; minimum: 256.5 mm) suggests that these effects largely determine Q in that period. Thus, this result suggests that, at least in KHEW, applying P and Q obtained in the same period to annual ET estimation might be inappropriate.

We examined the duration of continuous measurement required to obtain representative values of P and $P-Q_{WS3}$ for estimation of ET from the water budget, using the following three periods as the start of hydrologic year: 1 January, the start of the calendar year; 1 March, the rough date of the lowest Q_{WS3} ; and 1 September, the end of the summer when soil water content near the surface layer tends to be at a local minimum (Fig. 5). In both P and $P-Q_{WS3}$, large differences indicated high inter-annual variability. However, while differences in P between 2 years were similar to those over 3 or 4 years if the hydrologic year began in winter, the difference in $P-Q_{WS3}$ between 2 years was still relatively large. This is because P in the months preceding the period of $P-Q_{WS3}$ affected Q_{WS3} at the beginning of the period, and P occurring at the end of the period could be stored in the watershed and thus did not always directly affect Q_{WS3} until after the end of the period. Thus, a data series of 1–4 years was not enough to estimate average $P-Q_{WS3}$ because of large potential differences in the maximum and minimum estimations. This also supported the uncertainty of annual ET estimation from water budget as pointed out in Wilson et al. (2001) and Kosugi and Katsuyama (2007). Meanwhile, applying the 9-year $P-Q_{WS3}$ result could exclude the effect of dividing the period and that of time difference between P and

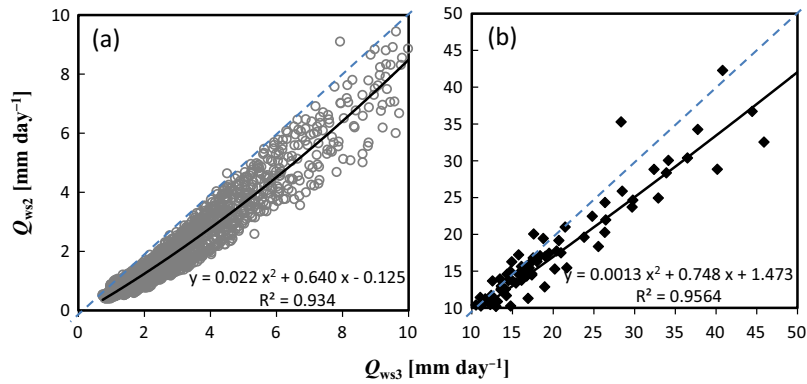


Fig. 3. Comparison between the daily runoff from WS2 (Q_{WS2}) and that from WS3 (Q_{WS3}) in the analysis period of this study (2001–2008); (a) $Q_{WS3} < 10 \text{ mm d}^{-1}$, and (b) $Q_{WS3} > 10 \text{ mm d}^{-1}$, respectively. A 1:1 line is also shown in each figure.

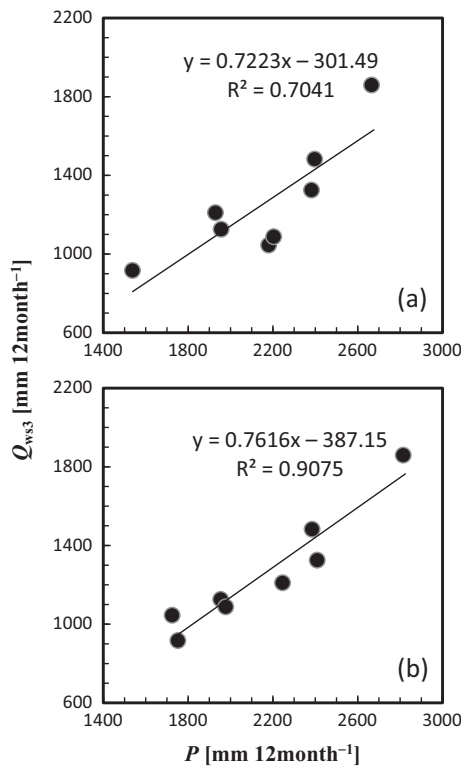


Fig. 4. Comparison of annual runoff from WS3 (Q_{WS3}) in the calendar year with 12 months of total rainfall (P): (a) Both P and Q_{WS3} were obtained in January–December, (b) 12 months of P was obtained from the previous year's September.

Q_{WS3} from ET estimation to some extent. Therefore, in this study we assumed that the 9-year average $P-Q_{WS3}$ ($= 897.5 \text{ mm}$) could be the representative value of ET estimated from the water budget measurement at KHEW. Surely, the value is a 9-year average and it is difficult to compare it directly with ET in 2007 and 2008, but it would become a reference index, considering that P in both years were within 10% range of the 9 year average P .

3.1.2. ET from eddy covariance method

Table 2 provides the annual values of ET_{EC} with energy imbalance correction ($ET_{EC,C}$), ET_{EC} without the correction ($ET_{EC,NC}$), and ET_{EC} calculated from the residual of the heat budget ($ET_{EC,R}$: $R_n - G - H - S_H$). The ET values estimated in Kuma14 and yearly water budget are also included in the table as references. The values of C_{IB} for daylight hours became low in winter when ET_{EC} was low and

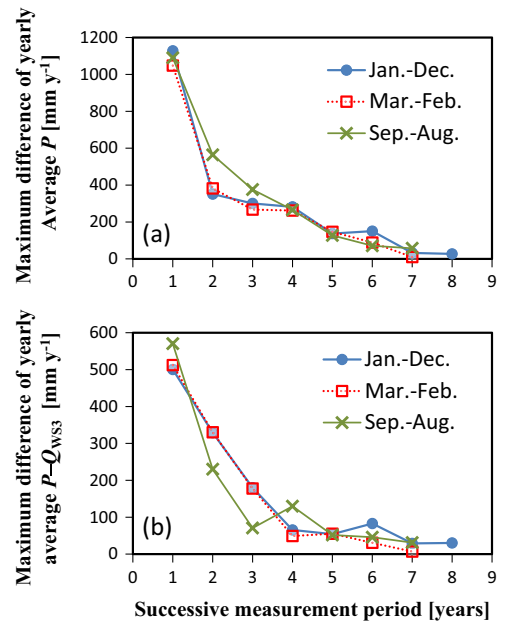


Fig. 5. Differences in average P (a) and $P-Q_{WS3}$ (b) between maximum and minimum estimates. The periods from January–December (closed circles), March–February (open squares) and September–August (crosses) were used to represent the hydrologic year.

high in summer when ET_{EC} was high (Fig. 6). Without accounting for wind direction, C_{IB} values for daylight hours were nearly equal to those of the right stream because of the dominant wind direction. Thus, $ET_{EC,C}$ would tend to be overestimated if calculated without classification of the wind direction (Table 2). Nighttime C_{IB} values were between 0.5 and 1.5 with a few exceptions.

The difference in the values of $ET_{EC,NC}$ between the right and left stream banks was large, as in Table 2 and Fig. 7a. The large difference was considered reasonable to some extent, because overstory vegetation apparently grew more vigorously on the right bank. Furthermore, slightly larger H on the left bank (Fig. 7b) and higher potential solar radiation on the left, south-facing bank suggested that the difference was neither strongly affected by a systematic error, such as advection caused by the complex topography, nor related to the input of solar energy. However, when using $ET_{EC,NC}$, we must assume huge leakage occurred even from WS3, because the value was much lower than the 9-year average of $P-Q_{WS3}$ ($= 897.5 \text{ mm}$). Meanwhile, by adopting $ET_{EC,R}$ calculated from the residuals of the heat budget, the values became

Table 2

Yearly evapotranspiration (ET) estimated on the basis of the eddy covariance method (ET_{EC}). The estimation processes are described in Table 1. The upper values outside the brackets and lower values correspond to the ET_{EC} calculated with and without wind direction categorization respectively. ET_{EC} from the left bank side and the right bank side are put left and right in the brackets. Results of water budget ($P-Q_{WS3}$) and ET by components sum (ET_{COMP} , April 2007–March 2008; Kumagai et al., 2014) are included as references.

Year	Energy imbalance corrected ($ET_{EC,C}$)	No correction ($ET_{EC,NC}$)	Residual of heat budget equation ($ET_{EC,R}$)	$P-Q_{WS3}$	ET_{COMP} (I_C : Interception loss, E_{UC} : Upper canopy transpiration, E_{SC} : Sub canopy evapotranspiration)
2007	839.9 (799.3, 880.5)	706.5 (608.5, 804.5)	925.6 (914.8, 936.4)	830.9	911.4 (425.2, 359.3, 126.9)
	862.5	794.7	915.2		
2008	811.8 (766.7, 856.9)	711.6 (646.8, 776.4)	892.1 (857.0, 927.2)	1116.1	
	861.9	786.1	916.2		

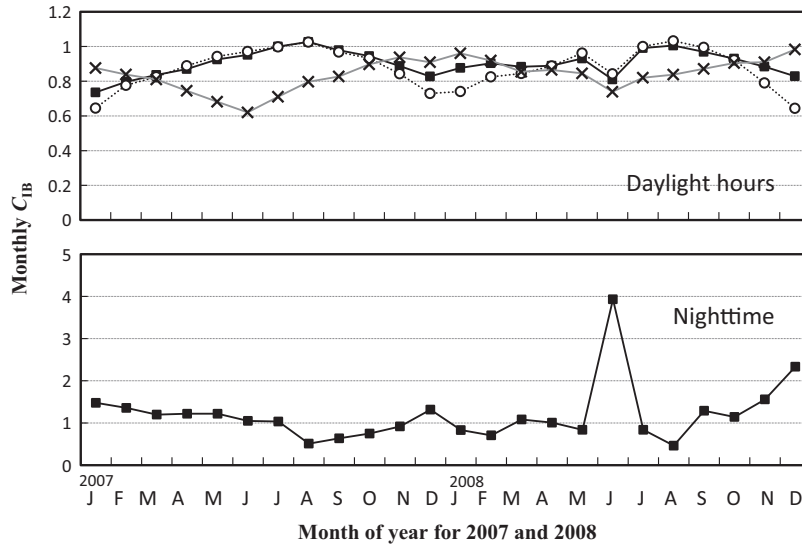


Fig. 6. Monthly energy imbalance correction coefficients (C_{IB}). Upper and lower panels are daylight hours and nighttime values, respectively. In the upper panel, open circles are values for the right bank, crosses represent left bank values, and closed circles are values calculated without classification by wind direction. Nighttime eddy fluxes are assumed to be similar in both bank sides.

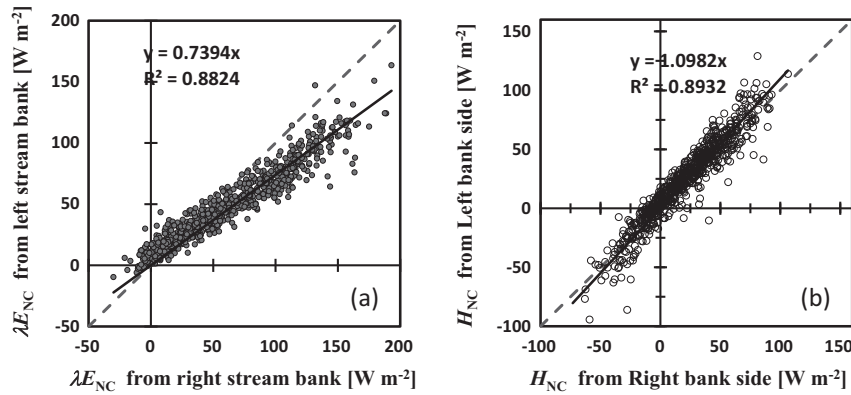


Fig. 7. Comparison of daily averaged eddy covariance latent heat flux (λ_{EC}) and sensible heat flux (H) calculated as the right bank data and those calculated as the left bank data without energy imbalance correction. Solid and dashed lines are regression line (zero offset was set) and 1:1 line, respectively.

closer to the 9-year average of $P-Q_{WS3}$. However, uncertainty remained because the values of $ET_{EC,R}$ for the left bank became similar to those of the right bank. The result induced a similar H from both banks. However, it might contradict the difference in observed ET, which might be related to the difference in the main planted species and their growth rate.

The values of $ET_{EC,C}$ were intermediate between $ET_{EC,NC}$ and $ET_{EC,R}$. $ET_{EC,C}$ is regulated by the value of R_n-G . Thus, the differences in $ET_{EC,C}$ between those calculated as the average of values

from the left and right banks and those estimated without the data divided by wind direction, and between those for the left bank and for the right bank, were lower than those in $ET_{EC,NC}$. However, even after the correction, $ET_{EC,C}$ calculated for the right bank was much higher than that for the left bank (Table 2).

In some studies, an energy imbalance correction was not necessarily required when focusing on the annual total ET_{EC} (e.g., Wilson et al., 2001; Scott, 2010). In addition, some researchers have concluded that the application of $ET_{EC,C}$ is necessary, because the

Table 3
Approximate values of tree density, percentage of measured throughfall (T_F) and stemflow (S_F) and calculated interception loss (I_C) to the measured rainfall (P) for each interception plot. Total values of each measurement period were also noted in the bracket.

Plot number	Approx. density (trees ha ⁻¹)	P (mm)	T_F (mm) (T_F/P)	S_F (mm) (S_F/P)	I_C (mm) (I_C/P)
Plot 1	1200	2835.0 ^a	2034.2 (0.718)	201.5 (0.071)	599.3 (0.211)
Plot 2	1600	1202.0 ^b	872.3 (0.726)	113.6 (0.094)	216.1 (0.180)
Plot 3	600	1631.0 ^c	1335.6 (0.819)	43.8 (0.027)	252.2 (0.154)

The periods of measurement which were successfully conducted are:

^a January 2007–May 2008 for plot 1.

^b January 2007–September 2007 except July 2007 for plot 2.

^c July 2007–May 2008 except September & November 2007 and April 2008 for plot 3.

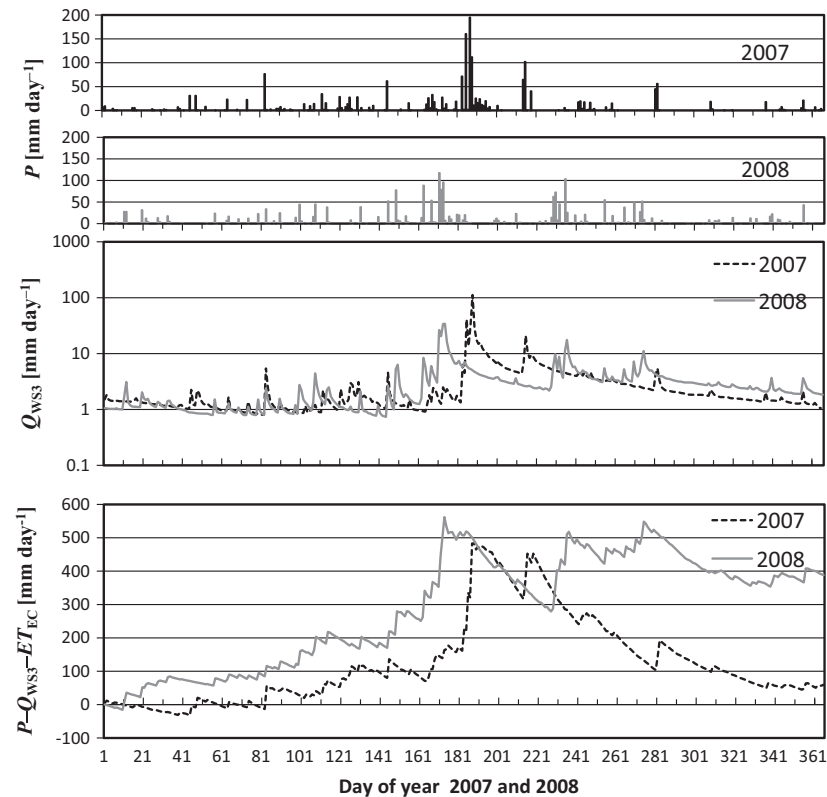


Fig. 8. Year-round rainfall (P), runoff from WS3 (Q_{WS3}), and early cumulative water storage in the watershed calculated by $P-Q_{WS3}-ET_{EC}$ in 2007 and 2008.

energy imbalance correction made ET almost equal to $P-Q$ (e.g., Ding et al., 2010; Barr et al., 2012). Meanwhile, Matsumoto et al. (2011) obtained P , Q and $ET_{EC,C}$ for 8 years at their forest watershed in Japan, and they suggested that 5.6% of P would be lost as bedrock infiltration on average. If we adopt the average $ET_{EC,C}$, this might be the case with our site. Comparing the average $ET_{EC,C}$ over the 2-year period of 2007 and 2008 (825.9 mm) with the 9-year averages of P and Q_{WS3} , the values of $P-Q_{WS3}-ET$ also became 0.034 P .

3.1.3. Interception loss plus sap-flow transpiration: confirmation of annual ET_{EC}

Table 3 shows the total measured T_F and S_F and estimated I_C from Eq. (2) for each plot with a successfully measured time period and approximate values of tree density. The ratio of T_F to P was smaller in plot 1 and plot 2 than in plot 3, and the ratio of S_F to P was the largest in plot 2, the plot with the highest tree density. The highest ratio of I_C to P (I_C/P) was found in plot 1, although

the tree density in plot 1 was intermediate between plots 2 and 3. Furthermore, compared with I_C/P expected from tree density (Komatsu et al., 2008; see also Kuma14), the values became larger in plot 1, and slightly smaller in plots 2 and 3. These results may be caused by the understory vegetation. Manfroi et al. (2006) reported that the understory trees change I_C/P by 3.5% in their tropical forest site. Among our interception plots, the understory vegetation flourished in plot 1 as well as other middle density Japanese cedar stands (e.g., UP and SP of sap-flux measurement plots) and this would result in increasing I_C/P .

Continuous I_C data were obtained only in plot 1. The vegetation of plot 1 was considered a representative Japanese cedar forest stand typical of those in KHEW, whereas plot 3 had exceedingly large Japanese cedar trees in the stand at this site. Thus I_C obtained in plot 1 was adopted in Kuma14 and combined the transpiration of $E_{UC} + E_{SC}$, to estimate ET for Japanese cedar forests in KHEW. As a result, the annual total value of ET_{COMP} ($= I_C + E_{UC} + E_{SC}$) from April 2007 to March 2008 was 911.4 mm; the distribution of I_C , E_{UC} and

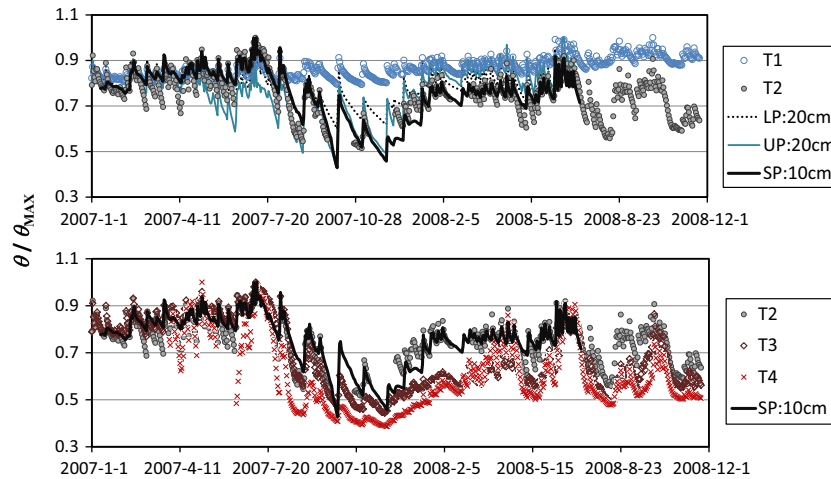


Fig. 9. (a) Seasonal variation of daily volumetric water content (θ) divided by each maximum value (θ_{MAX}) at the depth of 0.05 m for T1–T4 (from the valley to the left bank ridge), 0.1 m and 0.2 m for SP (middle of the slope in the left bank), and 0.2 m for UP (middle of the slope in the right bank) and LP (near the valley). See also Fig. 1b and c.

E_{SC} was 425.2 mm, 359.3 mm and 126.9 mm, respectively. ET_{COMP} was higher than total $ET_{EC,C}$ (842.9 mm) and slightly higher than $ET_{EC,C}$ from the right bank (875.2 mm) that was mainly occupied by Japanese cedar. Because the maximum I_C/P was observed in plot 1 among the three plots, and the right bank side includes plot 3 near LP as well as Japanese cypress stands although they are relatively small parts, the difference of 36.2 mm year⁻¹ is considered reasonable. Furthermore, when accumulated $ET_{EC,C}$ from the right bank was obtained when the downward solar radiation was greater than 0, the 12-month total became 894.1 mm and the difference from ET_{COMP} became close to 1.9%. We believe that the ET_{COMP} reliably represents ET from the Japanese cedar stands. Because one of the main factors, E_{UC} , was measured directly, and another main factor, I_C , was calculated by a simple and reliable method from the measurement of P , T_f and S_f , although we could not capture accurately when the intercepted water was vaporized to the atmosphere over the forest. Thus, the small difference indicates that the annual total $ET_{EC,C}$ calculated as that from the right stream bank is also reliable, and also indicates that the energy imbalance correction in ET_{EC} was appropriate for our site. The value of $ET_{EC,C}$ from the right bank was compatible with the estimation from BREB method in 1990s at this site (Shimizu et al., 2003). The BREB measurement had been carried out near the Japanese cedar forest canopy in WS3, and the estimated ET, typically 875 mm and 902 mm for the two tower observation sites, would also be representative of ET from Japanese cedar forest stands in KHEW. These facts imply that the potential ET from the planted conifers in the region would be about ≥ 900 mm. The value might actually be slightly smaller, because some soil water drained and concentrated near the valley, while some dried near the ridge.

3.2. Spatial and temporal variation in ET_{EC}

Values of P , Q_{WS3} , and $P - Q_{WS3} - ET_{EC,C}$ over the 2 years in which $ET_{EC,C}$ was estimated (2007 and 2008) are shown in Fig. 8. The variability between yearly $P - Q_{WS3}$ is well-illustrated by the values of $P - Q_{WS3}$ in 2007 and 2008 (830.9 mm and 1116.1 mm, respectively). The difference of 285.2 mm between years is too great to be caused by ET, as the difference in P between 2007 and 2008 was only 247.5 mm. By the end of 2007, $P - Q_{WS3} - ET_{EC,C}$ had returned to nearly zero, suggesting that water storage and leakage were negligible that year. However, Q_{WS3} was lower at the end of 2007 than at the beginning of the year, implying decreased soil water storage. In 2007, more than 35% of annual P occurred during

a 20 day period (22 June–11 July; day of year (DOY) 173–192); thus Q_{WS3} in DOY 180–229 in 2007 was higher than that in 2008 (Fig. 8b). The large value of P over a short timespan nearly saturated the soil in the watershed, as depicted by Fig. 9a and b, which shows the seasonal variation in θ/θ_{MAX} at each slope position using the values of SP or T2 as the standard (both were at nearly the same position). Under this highly wet condition, areas of soil water storage within the watershed would be connected, establishing a network of flow pathways that drain into the stream (e.g., Noguchi et al., 1999; Sidle et al., 2000). From late summer to early autumn when both the drainage from the pathway and ET were large, the θ/θ_{MAX} at the Japanese cypress plots (T3 and T4) became lower than at SP or T2 and stayed at that level. In 2007 in particular, lower autumnal P values may have caused soil dryness and subsequent disconnection of the throughflow pathways in the soil. In DOY 1–140 of 2008, rainfall was largely stored in the soil rather than contributing to runoff, although periodical P was slightly higher than P in the same period of 2007. Variation in soil water storage may be key to explain why the timing of Q was somewhat decoupled from P .

Low values of θ/θ_{MAX} in early 2008 relatively swiftly recovered near the lower and middle slope positions of Japanese cedar stands (Fig. 9a), while recovery was slow in the Japanese cypress stands (Fig. 9b). This difference might be partly caused by soil water repellency on the dry soil surface. This phenomenon sometimes emerges in KHEW, particularly in stands of Japanese cypress, although the repelled water usually infiltrates the soil through partially existing macropores and does not cause continuous overland flow (Kobayashi and Shimizu, 2007). Furthermore, Japanese cypress is much more sensitive to a lack of soil water content than Japanese cedar and tends to control transpiration under dry soil conditions (Nagakura et al., 2004). Accordingly, these characteristics may account for the difference between ET in the right bank, which is dominated by Japanese cedar, and that of the left bank, where Japanese cypress occupies a greater area.

The 2 years of ET_{EC} data were almost the same overall. However, as shown in Table 2, ET_{EC} in 2007 was slightly higher than that in 2008 regardless of the ET_{EC} estimation processes. Considering that P in 2007 was 12% lower than that in 2008 and monthly I_C was often proportional to monthly P (Komatsu et al., 2007; see also Figure of Kuma14), the unexpected results should be attributed mainly to vegetation transpiration being affected by other meteorological and hydrological factors. Fig. 10 shows the comparison of monthly variations of $ET_{EC,C}$ from both bank sides with R_n , T_a , D ,

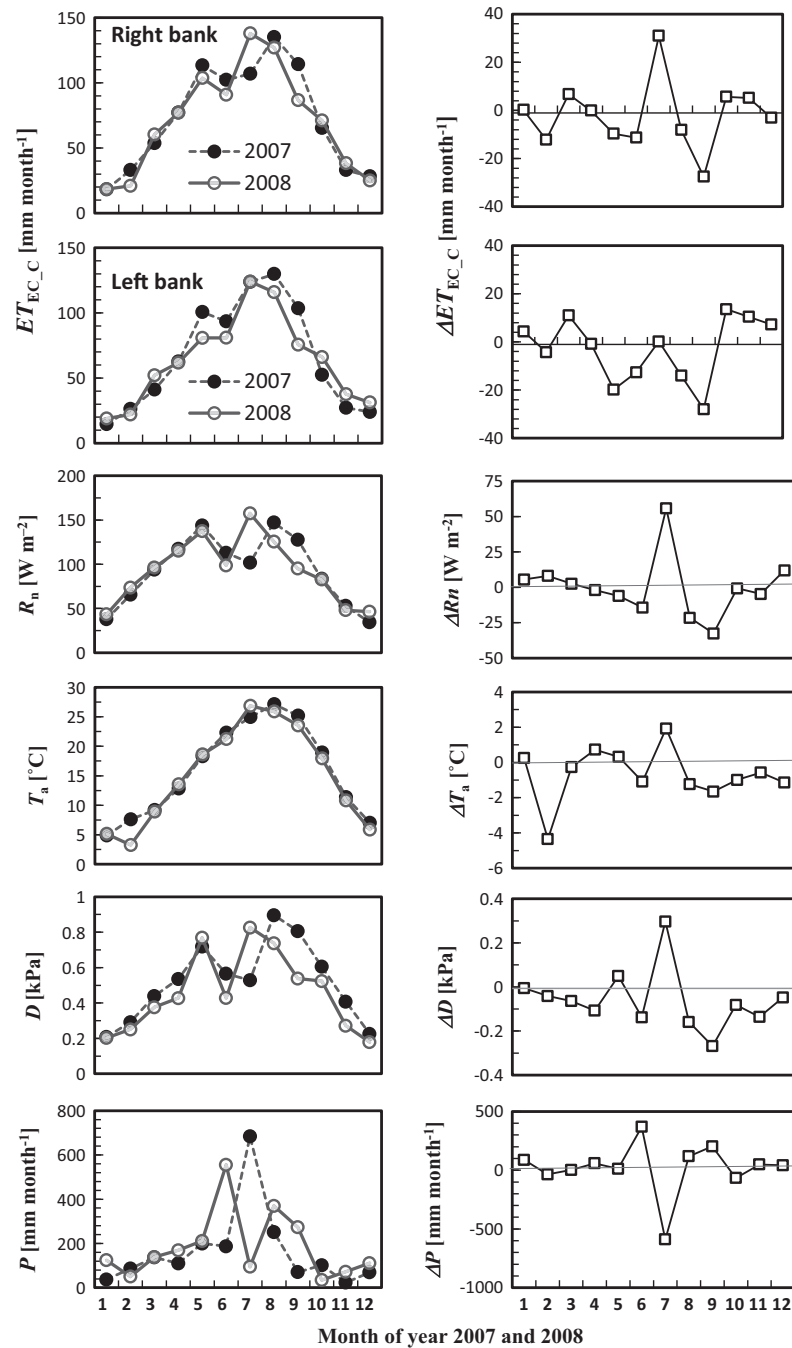


Fig. 10. Comparison of monthly evapotranspiration calculated using the eddy covariance method with a correction for energy imbalance (ET_{EC_C}) on the right bank (uppermost panels) and left bank (second upper panels) with meteorological factors in left side panels (2007: closed circles; 2008: open circles). Meteorological factors from the third upper panel to the lower: monthly averaged net radiation (R_n), air temperature at 42 m height (T_a), vapor pressure deficit at 42 m height (D), and monthly total rainfall (P). Right side panels are differences (Δ) in the same month's values between the 2 years (2008–2007).

and P . The right panels of Fig. 10 also show differences of these monthly values between 2007 and 2008 (ΔET_{EC_C} , ΔR_n , ΔT_a , ΔD , ΔP : Δ represents the residual of a certain value in 2008 subtracted from that in 2007). The seasonal variation of ET_{EC_C} from the right bank side was synchronized with that of D , R_n , and T_a , with R^2 ranging from 0.86 to 0.88. Correlations of ET_{EC_C} with these factors from the left bank, ranged from R^2 of 0.75–0.89. The correlation between ET_{EC_C} and monthly P was much lower ($R^2 = 0.24$ –0.34 for both sides of the bank): in both years, monthly ET_{EC_C} reached a maximum of about 4.0 mm day^{-1} in the next month after the maximum monthly P had occurred. The values of ΔET_{EC_C} in the right bank

also seem to have varied synchronously with ΔR_n and ΔD (R^2 of 0.72 and 0.59, respectively) but were less correlated with ΔT_a ($R^2 = 0.42$) and inversely correlated to ΔP ($R^2 = 0.65$). This was caused by an inverse correlation of increasing monthly P and decreasing monthly R_n . However, ΔET_{EC_C} in the left bank was not well-correlated with ΔR_n , ΔD and ΔT_a ($R^2 = 0.25$, 0.07, and 0.03, respectively), nor was there a strong inverse correlation with ΔP ($R^2 = 0.11$). These results suggest that ET_{EC_C} on both sides of the bank was strongly affected by radiative energy input, and the inter-annual difference in ET_{EC} between 2007 and 2008 was largely caused by the difference in radiative energy. Particularly on the

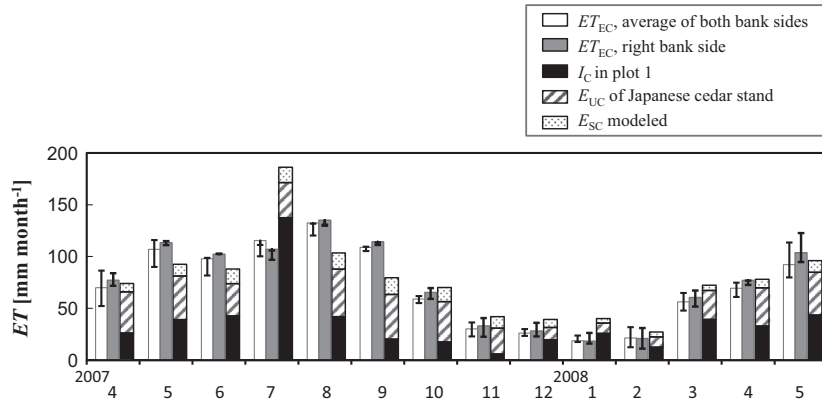


Fig. 11. Comparison of monthly total evapotranspiration (ET) from April 2007 to May 2008. White block and gray block are ET estimated by eddy covariance method with energy imbalance correction ($ET_{EC,C}$), average of data from both banks and the right bank, respectively. Error bars show the range from $ET_{EC,NC}$ (without energy imbalance correction) to $ET_{EC,R}$ (calculated as $R_n - G - H - S_H$). Black block, hatched block and pointed block are interception loss (I_C), Japanese cedar transpiration estimated from sap-flux measurement (E_{UC}) and understory transpiration from YPLANT model (E_{SC}), respectively.

right bank, ET_{EC} was determined by meteorological factors. However, on the left bank, the results imply that sub-factors may also control $ET_{EC,C}$. Soil water content may be one of the sub-factors, as total $\Delta ET_{EC,C}$ from January–July was lower on the left bank (−21.8 mm) than on the right bank (+4.3 mm), despite the lack of clear mutual correlation in the monthly values. From winter to spring of 2008, the difference in θ/θ_{MAX} in the Japanese cypress stands (T3 and T4) compared with the Japanese cedar stands (e.g., T2) was generally greater than the difference in the same period of 2007 (Fig. 9b), indicating drier soil conditions in that period of 2008. Furthermore, the reverse phenomena occurred from October–December, when total $\Delta ET_{EC,C}$ on the left bank (+31.3 mm)

was higher than that of the right bank (+7.7 mm) and θ/θ_{MAX} at T3 and T4 were similar to that of T2.

3.3. Differences between ET_{EC} and ET_{COMP} on a finer timescale

Although the annual $ET_{EC,C}$ from the right bank was similar to ET_{COMP} in Kuma14, the monthly variations suggest that the timing when maximum ET occurred was different between measurements based on ET_{COMP} and $ET_{EC,C}$ (Fig. 11). In the measurement period, the timing of maximum monthly ET_{COMP} occurred in July 2007 and was synchronized with maximum monthly P . Meanwhile, the maximum monthly $ET_{EC,C}$ was observed a month later, in

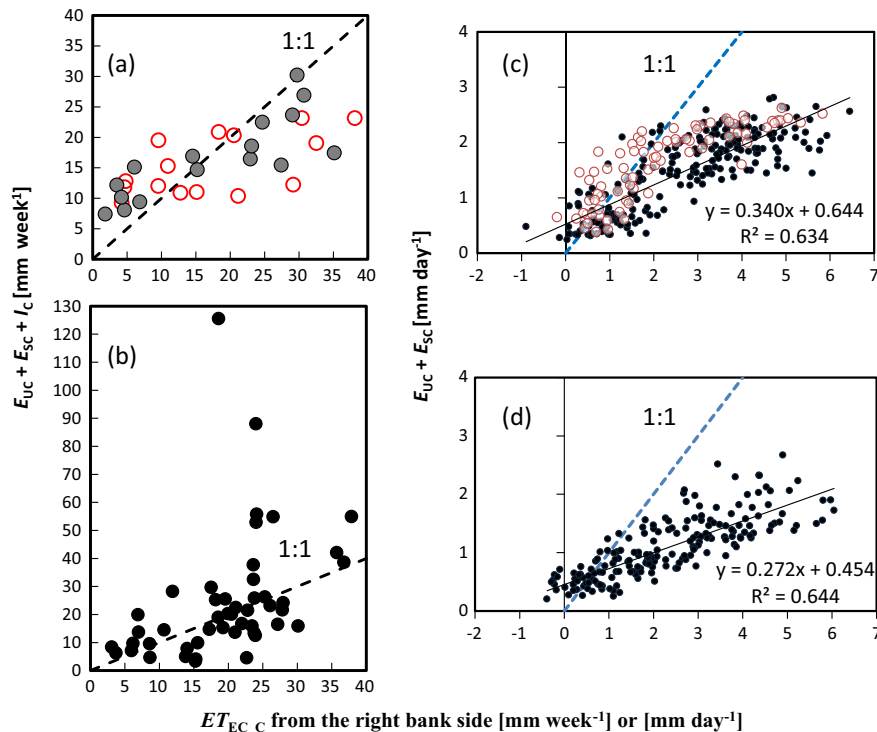


Fig. 12. Comparison of evapotranspiration (ET) from eddy covariance method ($ET_{EC,C}$) in the right bank with the ET components (E_{UC} : sap-flux transpiration, E_{SC} : modeled sub-canopy transpiration, and I_C : interception loss) observed in Japanese cedar plots. Left and right panels are weekly and daily comparisons. The upper and lower panels correspond to dry and wet conditions, divided by 20 mm rainfall week^{−1} (weekly: a and b), and with or without rain (daily: c and d), respectively. The open circles in the upper panels are very dry days, with less than 2 mm rain in the week (a) and no rain in the previous 5 days (c).

August 2007, when R_n reached its maximum. The difference might be partially caused by instrumental error. In wet conditions when the vapor pressure deficit became small, the correction of the closed-path ET_{EC} became greater (Ibrom et al., 2007), but the degree of correction might be insufficient because other instrument data used to determine the correction might become unreliable under these conditions. The results showing that C_{IB} became lower in winter than in summer might suggest the existence of some additional error under wet conditions, since D in winter decreases compared with that during the day in summer. Under a heavy rainfall event, the possibility of water overflow from the tipping buckets of the I_C measurement system would be also increased, although our data in plot 1 did not suggest this occurred.

However, this result did not depend on the regulation of R_n – G through the energy imbalance correction, as the values of C_{IB} were almost unity around the summer in 2007. Furthermore, the monthly values of ET_{-EC} from the right bank and those of ET_{COMP} were well matched except in July 2007 (Fig. 11). Thus, we performed weekly and daily comparison. During weeks in which P was less than 20 mm and ET_{EC-C} was more than 15 mm, ET_{EC-C} in the right bank was usually higher than ET_{COMP} (Fig. 12a). In weeks where P was higher, this trend changed slightly. Regardless of the ET_{EC} value, the weekly ET_{COMP} was frequently higher than ET_{EC-C} (Fig. 12b), and sometimes the difference was extreme. If this trend was caused by an error, it may be overestimation of weekly I_C and underestimation of weekly evaporation, which are included in E_{SC} . On a monthly basis, these errors compensated for one another, except when monthly P was extremely high as in July 2007. A comparison of the daily data showed a similar trend. As in Fig. 12c and d, ET_{EC-C} was generally much higher than $E_{UC} + E_{SC}$ on dry days when no rain was observed, as well as on wet (or rainy) days where daily ET_{EC-C} was larger than 2 mm. Additionally, when the comparison was limited to very dry days, after no rain was observed for 5 days including the day of observation, ET_{EC-C} values were sometimes nearly equal to $E_{UC} + E_{SC}$, although sometimes they became much higher. Considering that the total difference between ET_{EC-C} and $E_{UC} + E_{SC}$ was nearly equal to total I_C , the result implied that, on a dry day, I_C might occasionally be a significant part of ET_{EC-C} . Based on this assumption, the difference of the timing of ET_{EC-C} and ET_{COMP} may be caused by I_C calculated from Eq. (2): We could measure P , T_F and S_F in real time, but it did not mean that we could observe when intercepted P evaporated into the atmosphere. We can assume trees with thick bark, such as Japanese cedar and Japanese cypress, have a large surface area where water can attach (e.g. Iida et al., 2005). Some part of rainfall can attach to trees, and water from fog, part of which is produced in the form of droplets (Murakami, 2006), may also attach to the trees and forest floor, without being detected as T_F or S_F . Certainly, the cause of the difference in timing of the maximum ET was not determined in this study. However, to our knowledge, only a few studies presented the seasonal variation of I_C ($+E_{UC} + E_{SC}$) and ET_{EC} , both of which were simultaneously measured (e.g. Oishi et al., 2008). We hope the following study results will be reviewed soon by the scientific community, to clarify whether or not this type of disagreement usually occurs and what causes it to occur.

4. Concluding remarks

We calculated ET using the eddy covariance method as adapted for patchy plantation forests in southwestern Japan. Values ranged from 707 to 926 mm in 2007 and 712–893 mm in 2008. Through comparison with water budget results (P – Q) and interception loss plus vegetation transpiration ($ET_{COMP} = I_C + E_{UC} + E_{SC}$), we determined that ET_{EC} corrected with energy imbalance (ET_{EC-C}) would be the typical ET for our site; the values were 839.9 mm in 2007 and 811.8 mm in 2008. The difference in the 9-year average of

annual P – Q (897.5 mm) from ET_{EC-C} was about 3.5% of P , and it could be regarded as reflecting the effects of bedrock infiltration. Compared with ET_{COMP} of Japanese cedar forest stands and ET_{EC-C} from the right bank mainly occupied by Japanese cedar forest stands when solar radiation was greater than 0, the difference of annual total ET became 17.3 mm (1.9%). This result indicates that the process of downscaling ET_{EC-C} was successfully carried out in this study and this technique was appropriate for the estimation of annual ET from a forest stand scale even over a complex terrain.

The maximum monthly ET_{EC} co-occurred with the maximum R_n , and the maximum monthly ET_{COMP} and the maximum P co-occurred as well. The same kind of difference in the timing between the occurrence of ET_{EC} and ET_{COMP} was observed at our site. Because the dry canopy ET_{EC-C} was sometimes much higher than $E_{UC} + E_{SC}$, we considered the possibility that some P attached to the tree bark and some fog water often seen under the canopy during the rainfall slowly evaporated to the atmosphere.

The spatial variations of ET, represented as the difference in ET between the right and left stream banks, would be caused by the difference of species, and the water conditions regulated by the terrain and the seasonal distribution of rainfall. Through the examination of meteorological factors, we found the seasonal and the inter-annual variation of ET_{EC} was largely governed by radiative energy, although some undetermined sub-factors may partially affect ET.

Comparison of the ET estimation methods showed that each method has advantages and disadvantage at different temporal scales. ET_{COMP} includes I_C , which is robust measurement of water loss, but it is usually assumed that all I_C occurs rapidly after (or during) rain, which cannot be detected from the current method of I_C measurement. On the other hand, ET_{EC} may miss rapid interception loss because of limitations in the system of measurement. Water budget P – Q is more or less affected by leakage, and it is influenced by longer-term storage changes that occur on the order of months to a year. Therefore, data from each method must be considered at the appropriate time scale.

Acknowledgements

Maintenance of the KHEW is supported by the Kyushu Research Center of the Forestry and Forest Products Research Institute (FFPRI) and the National Forests in Kyushu Office. This work was financially supported by the Ministry of Agriculture, Forestry and Fisheries, Japan through a research project entitled “Development of technologies for mitigation and adaptation to climate change in Agriculture, Forestry and Fisheries (A-8)” and also supported by Grants-in-Aid for Scientific Research (Nos. 17380096 and 17510011) from the Ministry of Education, Science and Culture, Japan. The authors are grateful to Prof. Masakazu Suzuki of The University of Tokyo, Prof. Delphis F. Levia of The University of Delaware, and Dr. Kazuki Nanko of FFPRI for support of this study. The authors also thank Dr. Yasuhiro Ohnuki and Dr. Shoji Noguchi of FFPRI for helpful instruction, and Dr. Hiroaki Hagino of FFPRI and Dr. Natsuko Yoshifuji of Kyoto University for providing field information. Further, we appreciate the thoughtful comments and advice of three anonymous reviewers.

Appendix A. Tipping bucket correction

To calibrate the data for throughfall (T_F) and stemflow (S_F), we carried out the laboratory test for all the tipping buckets used in this study. At first we checked the capacity for a single tipping at the static status (c_t) by dripping water using a 10 cc cylinder. The flow injection test was essentially the same as Iida et al. (2012): A steady water flow was generated between the tested tipping

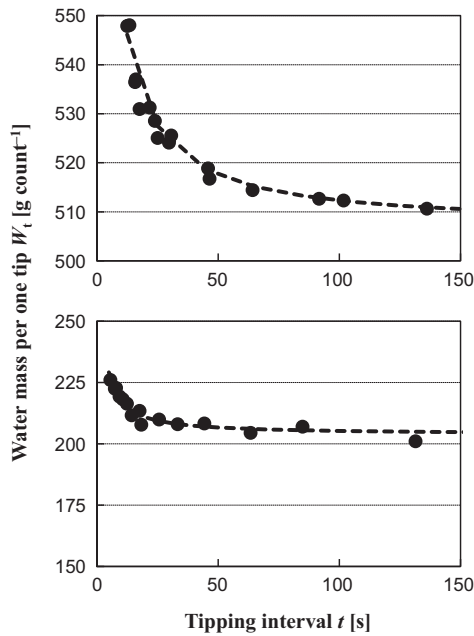


Fig. A1. Relationship between tipping interval (t) and water mass per one tip (W_t) obtained in the laboratory test for two tipping bucket flow meters. Upper and lower panels are 0.5-L type flow meter and 0.2-L type flow meter, respectively. The dotted-line curves are Eq. A1 parameterized for the flow meters.

bucket and a constant head bottle. The effluent from the bottle was initially collected by a storage tank set the same height of the tipping bucket, and it was measured by a graduated cylinder while the flow collecting time was measured by a stopwatch. Then the flow was injected to the tipping bucket and the time was measured for at least tipping twice. The process was continued with changing the flow rate, and then the parameters (p_1 , p_2 , p_3) of the following catenary curve were determined:

$$W_t = \text{MAX} \left(c_t, p_1 - \frac{p_2 t}{p_3 + t} \right) \quad (t < 3600), \quad (\text{A1a})$$

$$W_t = W_{3600} \quad (t > 3600), \quad (\text{A1b})$$

where t (s) is the averaged interval time between the tipping, W_t (mL) is the average injected water within t , $\text{MAX}()$ indicates the largest value within the bracket. Fig. A1 presented the examples of the results of laboratory test for the tipping buckets used in plot 1 in this study. The underestimation rate of uncorrected T_F and S_F were less than 4% for monthly data. For 17-month data obtained at plot 1, the underestimation would become 2.6% in total T_F and 2.3% in total S_F , respectively, and the underestimation would have induced overestimation of I_C by 9.6%.

References

- Barr, A.G., van der Kamp, G., Black, T.A., McCaughey, J.H., Nestic, Z., 2012. Energy balance closure at the BERMS flux towers in relation to the water balance of the White Gull Creek watershed 1999–2009. *Agric. For. Meteorol.* 153, 3–13.
- Domec, J.-C., Sun, G., Noormets, A., Gavazzi, M.J., Treasure, E.A., Cohen, E., Swenson, J.J., McNulty, S.G., King, J.S., 2012. A comparison of three methods to estimate evapotranspiration in two contrasting loblolly pine plantations: age-related changes in water use and drought sensitivity of evapotranspiration components. *For. Sci.* 58, 497–512.
- Ding, R., Kang, S., Li, F., Zhang, Y., Tong, L., Sun, Q., 2010. Evaluation eddy covariance method by large-scale weighing lysimeter in a maize field of northwest China. *Agric. Water Manage.* 98, 87–95.
- Dyer, A.J., 1974. A review of flux-profile relationships. *Boundary-Layer Meteorol.* 7, 363–372.

- Foken, T., Leuning, R., Oncley, S.P., Mauder, M., Aubinet, M., 2012. Corrections and data quality. In: Aubinet, M. et al. (Eds.), *Eddy Covariance: A Practical Guide to Measurement and Data Analysis*. Springer, Dordrecht, Heidelberg, London, New York, pp. 85–131.
- Ford, C.R., Hubbard, R.M., Kloeppel, B.D., Vose, J.M., 2007. A comparison of sap flux-based evapotranspiration estimates with catchment-scale water balance. *Agric. For. Meteorol.* 145, 176–185.
- Forestry Agency of Japan, 2013. Annual report on forest and forestry in Japan, fiscal year 2012. Zenkoku Ringyo Kairyu Fukyu Kyokai, Tokyo, p. 284 (in Japanese).
- Granier, A., 1987. Evaluation of transpiration in a Douglas-fir stand by means of sap flow measurements. *Tree Physiol.* 3, 309–320.
- Holst, J., Grote, R., Offermann, C., Ferrio, J.P., Gessler, A., Mayer, H., Rennenberg, H., 2010. Water fluxes within beech stands in complex terrain. *Intl. J. Biometeorol.* 54, 23–36.
- Hsieh, C.I., Katul, G., Chi, T., 2000. An approximate analytical model for footprint estimation of scalar fluxes in thermally stratified atmospheric flows. *Adv. Water Resour.* 23, 765–772.
- Hui, D., Wan, S., Su, B., Katul, G., Monson, R., Luo, Y., 2004. Gap-filling missing data in eddy covariance measurements using multiple imputation (MI) for annual estimation. *Agric. For. Meteorol.* 121, 93–111.
- Ibrom, A., Dellwik, E., Flyvbjerg, H., Jensen, N.O., Pilegaard, K., 2007. Strong low-pass filtering effects on water vapour flux measurements with closed-path eddy correlation systems. *Agric. For. Meteorol.* 147, 140–156.
- Iida, S., Tanaka, T., Sugita, M., 2005. Change of interception process due to the succession from Japanese red pine to evergreen oak. *J. Hydrol.* 315, 154–166.
- Iida, S., Ohta, T., Matsumoto, K., Nakai, T., Kuwada, T., Kononov, A., Maximov, T., van der Molen, M., Dolman, H., Yabuki, H., 2009. Evapotranspiration from understory vegetation in an eastern Siberian boreal larch forest. *Agric. For. Meteorol.* 149, 1129–1139.
- Iida, S., Shimizu, T., Kabeya, N., Nobuhiro, T., Tamai, K., Shimizu, A., Ito, E., Ohnuki, Y., Abe, T., Tsuboyama, Y., Chann, S., Keth, N., 2012. Calibration of tipping-bucket flow meters and rain gauges to measure gross rainfall, throughfall, and stemflow applied to data from a Japanese temperate coniferous forest and a Cambodian tropical deciduous forest. *Hydrol. Proc.* 26, 2445–2454.
- Ikawa, R., 2008. Quantitative evaluation of stemflow contribution to rainfall-runoff process in a mountainous forested area. Doctoral thesis of Kumamoto University, p. 45–49 (in Japanese).
- Katsuyama, M., Tani, M., Nishimoto, S., 2010. Connection between stream water mean residence time and bedrock groundwater recharge/discharge dynamics in weathered granite catchment. *Hydrol. Proc.* 24, 2287–2299.
- Kobayashi, M., Shimizu, T., 2007. Soil water repellency in a Japanese cypress plantation restricts increases in soil water storage during rainfall events. *Hydrol. Proc.* 21, 2356–2364.
- Komatsu, H., Tanaka, N., Kume, T., 2007. Do coniferous forests evaporate more water than broad-leaved forests in Japan? *J. Hydrol.* 336, 361–375.
- Komatsu, H., Maita, E., Otsuki, K., 2008. A model to estimate annual forest evapotranspiration in Japan from mean annual temperature. *J. Hydrol.* 348, 330–340.
- Kosugi, Y., Takanashi, S., Tanaka, H., Ohkubo, S., Tani, M., Yano, M., Katsuyama, T., 2007. Evapotranspiration over a Japanese cypress forest. I. Eddy covariance fluxes and surface conductance characteristics for 3 years. *J. Hydrol.* 337, 269–283.
- Kosugi, Y., Katsuyama, M., 2007. Evapotranspiration over a Japanese cypress forest. II. Comparison of the eddy covariance and water budget methods. *J. Hydrol.* 334, 305–311.
- Kumagai, T., Aoki, S., Shimizu, T., Otsuki, K., 2007. Sap flow estimates of stand transpiration at two slope positions in a Japanese cedar forest watershed. *Tree Physiol.* 27, 161–168.
- Kumagai, T., Tateishi, M., Miyazawa, Y., Yoshifuji, N., Komatsu, H., Shimizu, T., 2014. Estimation of annual forest evapotranspiration from a coniferous plantation watershed in Japan (1): water use components in Japanese cedar stands. *J. Hydrol.* 508, 66–76.
- Manfroi, O.J., Kuraji, K., Suzuki, M., Tanaka, N., Kume, T., Nakagawa, M., Kumagai, T., Nakashizuka, T., 2006. Comparison of conventionally observed interception evaporation in a 100-m² subplot with that estimated in a 4-ha area of the same Bornean lowland tropical forest. *J. Hydrol.* 1–2, 329–349.
- Matsumoto, K., Kosugi, Y., Katsuyama, M., Tani, M., Ohkubo, S., Takanashi, S., 2011. Estimation of bedrock infiltration on a weathered granitic mountain covered by Japanese cypress forest using water-budget and eddy covariance methods. *Intl. J. Erosion Control Eng.* 4, 10–20.
- McGlynn, B., McDonnell, J., Stewart, M., Seibert, J., 2003. On the relationship between catchment scale and mean residence time. *Hydrol. Proc.* 17, 175–181.
- Murakami, S., 2006. A proposal for a new forest canopy interception mechanism: splash droplet evaporation. *J. Hydrol.* 319, 72–82.
- Nagakura, J., Shigenaga, H., Akama, A., Takahashi, M., 2004. Growth and transpiration of Japanese cedar (*Cryptomeria japonica*) and Hinoki cypress (*Chamaecyparis obtusa*) seedlings in response to soil water content. *Tree Phys.* 24, 1203–1208.
- Noguchi, S., Tsuboyama, Y., Sidle, R.C., Hosoda, I., 1999. Morphological characteristics of macropores and the distribution of preferential flow pathways in a forested slope segment. *Soil Sci. Soc. Am. J.* 63, 1413–1423.
- Ohnuki, Y., Shimizu, A., 1998. Soil layer structure at the uppermost reach of Kahoku Experimental Watershed. *Bull. Kyushu Branch Jpn. For. Soc.* 51, 105–106 (In Japanese).

- Oishi, A.C., Oren, R., Stoy, P.C., 2008. Estimating components of forest evapotranspiration: a footprint approach for scaling sap flux measurements. *Agric. For. Meteorol.* 148, 1719–1732.
- Pearcy, R.W., Yang, W., 1996. A three-dimensional crown architecture model for assessment of light capture and carbon gain by understory plants. *Oecologia* 108, 1–12.
- Scott, R.L., 2010. Using watershed water balance to evaluate the accuracy of eddy covariance evaporation measurements for three semiarid ecosystems. *Agric. For. Meteorol.* 150, 219–225.
- Shimizu, A., Miyabuchi, Y., Takeshita, M., 1994. Some observations on the hydrological phenomena of the forest experimental watershed in a warm-temperate region. *Proc. Intl. Symp. For. Hydrol.* 1994, 367–374.
- Shimizu, A., Shimizu, T., Miyabuchi, Y., Ogawa, Y., 2003. Evapotranspiration and runoff in a forest watershed, western Japan. *Hydrol. Proc.* 17, 3125–3139.
- Shimizu, T., Suzuki, M., Shimizu, A., 1999. Examination of a correction procedure for the flow attenuation in orthogonal sonic anemometers. *Boundary-Layer Meteorol.* 93, 227–236.
- Shimizu, T., 2007. Practical applicability of high frequency correction theories to CO₂ flux measured by a closed-path system. *Boundary-Layer Meteorol.* 122, 417–438.
- Shimizu, T., Effect of coordinate rotation system on calculated fluxes over a complex terrain forest: a comprehensive comparison. *Boundary-Layer Meteorol.*, submitted for publication.
- Sidle, R.C., Tsuboyama, Y., Noguchi, S., Hosoda, I., Fujieda, M., Shimizu, T., 2000. Stormflow generation in steep forested headwaters: a linked hydrogeomorphic paradigm. *Hydrol. Proc.* 14, 369–385.
- Siebicke, L., Hunner, M., Goken, T., 2012. Aspects of CO₂ advection measurements. *Theor. Appl. Climatol.* 109, 109–131.
- Tamai, K., Shimizu, T., Ohnuki, Y., Ishizuka, S., 2010. Topographical variation of soil respiration in a warm-temperate evergreen forest in Kumamoto Prefecture, western Japan, Japan. *J. For. Environ.* 52, 1–10 (in Japanese with English abstract).
- Waichler, S.R., Wemple, B.C., Wigmosta, M.S., 2005. Simulation of water balance and forest treatment effects at the H.J. Andrews experimental forest. *Hydrol. Proc.* 19, 3177–3199.
- Webb, E.K., Pearman, G.I., Leuning, R., 1980. Correction of flux measurements for density effects due to heat and water vapour transfer. *Quart. J. Roy. Meteorol. Soc.* 106, 85–100.
- Wilson, K.B., Hanson, P.J., Mulholland, P.J., Baldocchi, D.D., Wullschlegel, S.D., 2001. A comparison of methods for determining forest evapotranspiration and its components: sap-flow, soil water budget, eddy covariance and catchment water balance. *Agric. For. Meteorol.* 106, 153–168.
- Yamashita, T., Kasuya, N., Nishimura, S., Takeda, H., 2004. Comparison of two coniferous plantations in central Japan with respect to forest productivity, growth phenology and soil nitrogen dynamics. *For. Ecol. Manage.* 200, 215–226.
- Zhang, L., Dawes, W.R., Walker, G.R., 2001. Response of mean annual evapotranspiration to vegetation changes at catchment scale. *Water Resour. Res.* 37, 701–708.